## A New Method for Predicting Rutting in Asphalt Pavements Employing Static Uniaxial Penetration Test

Kai Su<sup>1+</sup>, Li-jun Sun<sup>1</sup>, and Yoshitaka Hachiya<sup>2</sup>

Abstract: To accurately estimate rutting is an essential input for efficient pavement management systems. In the past, many efforts have been devoted to developing advanced rutting prediction models. However, a versatile prediction model for rutting is still being pursued by now because of poor suitability of the empirical procedures when exposing to extreme environmental conditions and heavy traffic loading. As the understanding of pavement materials behavior and structural models, mechanistic-empirical based procedures starts becoming increasingly more popular because they can overcome most of the technical limitations of purely empirical methods. The paper brings out a developed mechanistic-empirical model for predicting rutting in flexible pavements considering rutting resistance of pavement structure and materials, and also taking into account traffic and environmental characteristics. The most notable feature of this procedure is based on sound mechanistic principles efficiently considering shear factors, which employs shear strength to evaluate the resistance to deformation of asphalt mixture, and shear stress to reflect the load level applied to the interest pavement structure. An optimization approach based on accumulation of sub-layer deformation is used to determine the coefficients of prediction model through laboratory wheel tests at varying conditions, including different temperatures, pressures and slab thicknesses. In addition, the vehicle speed with pronounced effect on rutting is successfully introduced into the model by means of Boltzmann's superposition principle. Furthermore, additional asphalt mixtures are prepared to verify the model by wheel tracking test, which gives satisfactory results. At last, the model is calibrated using accelerated pavement test results.

Key words: Accumulation of sub-layer deformation; Rutting prediction model; Shear stress; Static uniaxial penetration test.

## Introduction

Rutting acknowledged as a common concern, loosely defined as longitudinal depressions in the wheel path accompanied by upheaves to the sides, is one of the major distresses formed in asphalt pavements, which usually results from the traffic loads at high temperature. The accurate prediction of their development is an essential input for the efficient management of pavement systems. In addition to their importance in making maintenance and rehabilitation decisions, properly specified pavement deterioration models can be used to study the effect of different loading levels and thus allocate cost responsibilities to various vehicle classes for their use of the highway system [1]. Furthermore, when such models play an important role in the mechanistic-empirical design method, they can also be used in the design of pavement structures (NCHRP, [2]). In particular, the models for predicting rutting can be used for evaluating different strategies for design, maintenance, and rehabilitation in pavement management systems.

Rutting in asphalt pavement is believed to be due to the combination of densification and shear flow of hot-mix asphalt (HMA), whereas most severe rutting is caused by the shear flow within the asphalt mixtures [3-6]. This is especially true for asphalt pavements compacted well during construction, in which the asphalt layer is responsible for most of the deformation. With the NCHRP

In years past, a number of pavement researchers favored the application of the shear concept to the design of asphalt concrete mix, instead of the visco-elastic approach [8-10]. However, research in this direction has not yet achieved widespread accepted result, probably due to the complexity of test methods, such as triaxial tests and repeated simple shear test at constant height. In addition, the triaxial test widely used in geotechnical engineering seems not to efficiently characterize asphalt concretes. A frequent question is how much of the actual confining pressure should be applied to calculate the shear strength in triaxial tests. No one can give a clear answer. In fact, the confining pressure varies at different positions along the depth in pavement. This condition has changed in recent years with the invention of the Static Uniaxial Penetration Test (SUPT) [11], a simple and compact but practical method for determining the shear resistance of asphalt concrete.

This paper presents a new approach to predicting rutting in asphalt pavements, which efficiently considers shear properties of pavement structure and materials realized by finite element method (FEM) analysis and SUPT test, respectively, and takes into account environmental and traffic characteristics, including load magnitude and repetitions plus vehicle speed. The model is validated by

Note: Submitted June 14, 2007; Revised September 14, 2007; Accepted September 18, 2007.

<sup>1-37</sup>A, completed in 2004, another encouraging finding was put forward by Mohamed et al. [7] that the rutting-depth relationship investigated from MnRoad sections was similar with that between shear stress and depth in pavement, which roughly indicated that a method to consider shear stress based on mechanics would be more reasonable to adjust the rutting as the function of depth within the asphalt thickness than the empiricism used in the current Mechanistic Empirical Design Guide (NCHRP [2]). In case of shear flow, both shear strength of HMA and shear stress in pavement play a key role for asphalt pavements to provide adequate resistance to rutting.

The Key Laboratory of Road and Traffic Engineering of Ministry of Education, Tongji University (No.1239, Siping Road, Shanghai, 200 - 0092, China)

Airport Research Center, Port and Airport Research Institute (3-1-1, Nagase, Yokosuka 239-0826, Japan)

<sup>&</sup>lt;sup>+</sup> Corresponding Author: E-mail <u>kai-su@pari.go.jp</u>

laboratory tests, and demonstrated using additional asphalt mixtures. Further applicability was achieved after implementing the calibration using accelerated pavement test results. This research aims to lay the foundation for putting forward appropriate design indexes to control rutting, and thus integrate asphalt mixture design within a structure design framework.

## Framework of Rutting Prediction Model

This study focuses on shear deformation induced by traffic-loads within the asphalt layer, without considering structural rutting due to the fact that densification is unlikely with well compacted HMA concrete pavements. In the past, much research [7, 12] indicated that this type of rutting was mainly associated with properties of pavement structure and materials, traffic characteristics such as load magnitude, vehicle speed and number of load repetitions, as well as temperature and humidity conditions. In general, prediction in the field rutting evolution is based on the empirical equation widely used in the United States (Harold and Von, [13]) [1, 7], which is expressed in terms of power function as shown in Eq. (1). This equation accounts for the incremental development of rutting over time as a function of load repetitions and temperature, where RD is the rutting depth after the load repetitions of N at the temperature of T.  $\alpha$ ,  $\beta$ , and  $\theta$  are the experimentally determined coefficients.

$$RD = \alpha \times N^{\beta} \times T^{\theta} \tag{1}$$

However, recent findings indicate that the exponent of load repetitions generally varies when exposed to different loads or using different materials [9, 14, 15], and that the value of  $\beta$  in Eq. (1) mainly depends on the magnitude of loads and properties of asphalt mixture. Therefore, it can be inferred that a constant value for  $\beta$  is not reasonable in this model, which often leads to typical empirical model failure in predicting rutting. In order to expand the scope of Eq. (1), the exponent should be adjusted to a function of load repetitions and materials properties to reflect the variability of loads and materials. Then, Eq. (1) is converted into Eq. (2):

$$RD = \alpha \times N^{\beta \cdot k} \times T^{\theta} \tag{2}$$

where  $k = (\tau/\tau_0)^\mu$ .  $\tau$ , shear tress, reflects the loading level applied to a given pavement structure, which can be calculated by finite element method, and  $\tau_0$  accounts for the shear strength of HMA determined by SUPT. Note that the ratio of  $\tau$  to  $\tau_0$  is denoted by parameter k and that  $\mu$  is the exponent for parameter k. Though  $\tau_0$  and  $\tau$  are all derived from elastic system, the ratio between  $\tau$  and  $\tau_0$  can minimize the system error resulting from using elastic theory for computing them. Herein, shear strength is only aimed at differentiating the shear resistance of different asphalt mixtures. Therefore, 60°C is designed as the tested temperature for the SUPT test. Resilient modulus at the temperature of 20°C is used to compute shear stress so that different pavement structures can be differentiated.

Vehicle speed greatly affects rutting evolution because of the viscous property of HMA; that is, lower speed results in greater rutting depth, just as found in slope section and intersection. However, it is very difficult to capture the relationship of deformation to speed, due to its complexity, and different researchers have given significantly different results for the effect of

speed on rutting [9, 16]. Therefore, the Boltzmann's superposition principle, suitable for linear visco-elastic materials [17], as an alternative method without the expense of precision, is used to consider the effect of vehicle speed on rutting; that is, the total deformation can be directly calculated by summing all the increments occurring at different times. For realizing this target, another important empirical equation is introduced, namely, that the loading duration of each load is the reverse of the vehicle speed [18]. So it can be deduced that the rutting depth caused by one application of a standard load with the speed of 10km/h is equivalent to the deformation caused by 10 performances of the standard load of 100km/h. On the basis of the previous analysis, the complete prediction model is illustrated in Eq. (3), where RD is the final rutting depth in mm,  $V_{ref}$  is the reference speed in km, V is the actual speed in km/h, and  $N_{\nu}$  is the number of load repetitions at the speed of V and the temperature of T in  ${}^{\circ}C$ .

$$RD = \alpha \times \left(\frac{V_{ref}}{V} \cdot N_{V}\right)^{\beta \cdot K} \times (T)^{\theta}$$
(3)

In reality, the shear stress, temperature and properties of HMA vary along the depth in asphalt pavement, which in turn results in different deformation at different sub-layer depth. For these reasons, the approach of accumulating all sub-layer deformations as the overall deformation, seems more rational and can significantly enhance the suitability of Eq. (3). In this study, the asphalt layer is divided into smaller sublayers with the thickness of 10mm, and the mid-depth of each sub-layer is adopted as the computational point. Thus, one can obtain the total rutting depth from Eq. (4) by simply summing all sub-layer rutting through the entire layer calculated, based on the actual shear stress, temperature and shear strength of asphalt concrete at different positions. In Eq. (4), i reveals the sub-layer position number and n represents the amount of sub-layer.

$$RD = \sum_{i=1}^{n} \Delta RD_i \tag{4}$$

Where  $\Delta RD_i$  stands for "the deformation of the *i* sub-layer".

## **Laboratory Experimental Program**

A series of laboratory tests, including the wheel tracking test, SUPT test and resilient modulus test coupled with finite element analysis (FEM), were conducted to determine the parameter coefficients of Eq. (4). The wheel tracking test was used to provide the data of rutting evolution with the load repetitions. The shear strength of HMA was decided by SUPT. To calculate the shear stress in the wheel tracking slab, the finite element model for tracking slab was built and the HMA resilient modulus required was also measured as an important input parameter.

## Wheel Tracking Test

Different wheel tracking devices have been used in different countries, such as the French pavement rutting tester, the Hamburg wheel tracking tester, the Georgia loaded wheel tester, the China wheel tracking tester, and so on. All these devices are somewhat similar in concept but differ slightly in design and operation [19].

In this study, testing was performed using the wheel tracking tester with a solid rubber-faced wheel specified in the current specification of China (JTJ052 [20]), in which the deformation can be recorded automatically and saved as an Excel file. This device was originally developed by British Transport Research Laboratory (TRL) in England [21]. It was capable of applying temperatures between 0 and 70°C, which were the lowest and highest temperature, respectively. The tire-specimen contact pressure can be applied up to 1.3MPa. Here, the maximum number of load repetitions was limited within 2520 passes with a constant speed of 0.58km/h. Additionally, it should be pointed out that the rutting formed in this type of rutting test, consisting of small densification and shear flow, was basically consistent with that found in the field.

#### **Static Uniaxial Penetration Test**

In the traditional triaxial test, the shear strength of asphalt mixtures can only be calculated through the Mohr-Coulomb principle, employing measured cohesion and angle of friction as well as normal effective stress. However, normal effective stress is closely related to confining pressure, which is a variable. Usually, shear strength is decided by using an assumed normal stress. Basically, shear strength as an intrinsic property of HMA, like modulus, is constant at a given condition. Therefore, the variance of the confining pressure limits the triaxial test to give a unique shear strength for asphalt concrete. Considering the complexity and deficiency, the Static Uniaxial Penetration Test (denoted SUPT) conducted on the Material Test System (MTS 810) was employed as shown in Fig. 1, which can directly determine the shear strength of HMA [22, 23].

First, the distributions of shear stress in the specimen perfectly agree with the distributions of shear stress in pavement structure when the same loads (single uniform circular) of 0.7MPa were applied (Fig. 2). Second, because the diameter of the loading rod is much less than the diameter of the specimen, the peripheral material will provide a confining pressure for the columned parts under the loading rod. The failure of the specimen is followed by the loss of confining pressure. Third, the confining pressure will be determined by the properties of asphalt cement and asphalt mixture at the

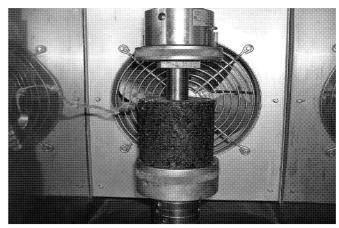


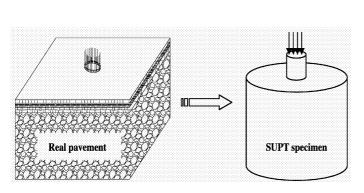
Fig. 1. Schematic Graph of Static Uniaxial Penetration Test.

position of maximum shear stress, and will increase with the increase of vertical penetration force, which leads to the mechanical response in SUPT, similar to real pavement structure.

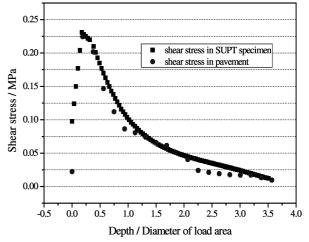
During this test, the loading head (steel rod with a diameter of 28.5mm) penetrates into the HMA specimen at a displacement controlled manner, with the loading rate of 1mm/min [22, 23]. The specimen size is 100mm in diameter by 100mm in height, which can be easily molded by a Superpave gyratory compactor. An environmental chamber was to maintain a constant specimen temperature of 60°C. The typical Loading-Deformation Curve in the SUPT test is shown in Fig. 3, where the pressure corresponding to the failure deformation point is defined as P used to calculate the ultimate shear strength. The shear strength obtained from the SUTP test was specified as Eq. (5):

$$\tau_0 = \overline{\tau} \cdot (P/A) \tag{5}$$

where  $\mathcal{T}_0$  is the shear strength of HMA, P is the axial load in kN at failure point, A is the cross section area in  $m^2$  of the steel loading rod and  $\overline{\mathcal{T}}$  is named as the strength coefficient with the suggested value of 0.339, determined by semi-infinitive space theory as explained below.



(a). UPT specimen and real pavement



(b). Shear stress distribution

Fig. 2. Comparison of Shear Stress Distribution in Specimen and Pavement Structure.

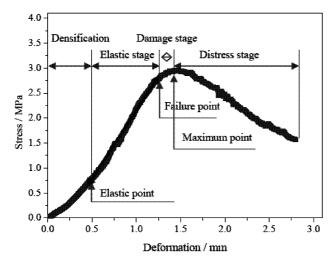


Fig. 3. Typical Loading-Deformation Curve of SUPT.

At the failure point in SUPT test as described in Fig. 3, the specimen just arrives at a balanced condition, in which the shear strength of HMA is equal to the maximum shear stress in the specimen. Meanwhile, through Eq. (5), it can be known that the strength coefficient can be decided by the shear strength of HMA, when the pressure (*P/A*) is 1MPa, which is described in Eq. (6).

$$\overline{\tau} = \frac{\tau_0}{1} = \tau_0 \tag{6}$$

Based on the above analysis, therefore, it can be deduced that strength coefficient ( $\overline{\tau}$ ) is equal to the maximum shear stress inside the specimen when 1MPa is applied. In addition, as previously stated, this test can simulate the real pavement when the diameter of the loading rod is much less than the diameter of the SUPT specimen. In other word words, the maximum shear stress in the SUPT specimen can be determined by Boussinesq theory in semi-infinitive space in term of Eq. (7) [17]. As a result, the calculated maximum shear stress is 0.339MPa when the Poisson ratio of the specimen is 0.35. Consequently, 0.339 is suggested as the strength coefficient.

$$\tau_{m} = \frac{p}{4} \left\{ (1 - 2\mu) + \frac{2(1 + \mu)\frac{z}{a}}{\left[ (1 + (\frac{z}{a})^{2})^{3/2} - \frac{(1 - 2\mu)(\frac{z}{a})^{3}}{\left[ (1 + (\frac{z}{a})^{2})^{3/2} \right]^{3/2}} \right\}$$
(7)

Bi [23] and Chen et al. [24] carried out a number of laboratory tests to evaluate the repeatability of SUPT. Test results indicated that the repeatability of SUPT can be considered acceptable, and that SUPT can efficiently differentiate the shear strength of different

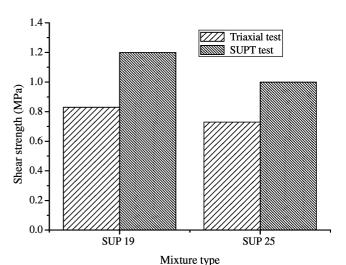


Fig. 4. Comparison of SUPT and Triaxial Shear Strength.

asphalt mixtures, verified by the fact that the rank of SUPT shear strength of HMA is identical to that measured by the triaxial test. Fig. 4 illustrates the compared results [24].

## **Resilient Modulus Test and 3-D FEM Model**

The HMA static compressive resilient modulus test, widely used in China, was relatively simple and was conducted on a specimen measuring 100mm in diameter by 100mm in height. The test was performed by applying a vertical load with the duration of 1sec to a cylindrical specimen, followed by removing the load with the recovering time of 30sec, and measuring the corresponding resilient deformation. Usually, the seven elevated loads, ranging from 0.4 to 0.7Mpa, were applied successively at intervals of 0.05MPa/level. The loading rate was maintained at a rate of 2mm/min. The compressive resilient modulus was defined as the slope in the plot of loads and resilient deformation.

Fig. 5 presents the FEM model with the same size as the wheel tracking slab sample, which was established to compute the shear stress in the wheel tracking slab. The displacement constraints conditions are listed below: the ZY and ZX plane was fixed in the X and Y directions, respectively, and other directions are free; the bottom side was completely fixed with constraints in the X, Y and Z directions. Again, it should be noted that, although both the shear strength coefficient and shear stress were determined by elastic mechanics theory, the ratio of shear strength to shear stress can furthest eliminate the errors caused by linear elastic assumption, in spite of visco-elastic seeming more reasonable to characterize the behavior of HMA.

 Table 1. Aggregate Gradations for Evaluated Asphalt Mixtures.

Sieve size (mm)	19	16.0	13.2	9.5	4.75	2.36	1.18	0.6	0.3	0.15	0.075
AC-13		100	97.5	79	58	44.5	32.5	24	17	12	6
Type A		100	95	70	48	36	24	18	12	8	4
Type B		100	97.5	79	58	39	29	22	15	10	5
Type C	100	95	75	58	42	32	22	16	11	7	4
Type D		100	95	62.5	27	20.5	19	16	13	12	10

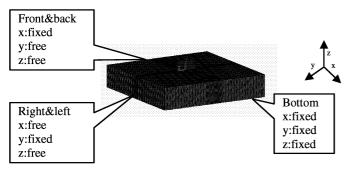


Fig. 5. FEM Model for Wheel Tracking Specimen.

# **Prediction Model Decided by Laboratory Tests Results**

#### **Test Results**

In the wheel tracking test, a typical asphalt mixture for surface course used in China, AC-13, was employed, and the aggregate gradation was illustrated in Table 1. Diabase was adopted as aggregates, and the asphalt binder used in this asphalt concrete was straight asphalt with the penetration of 60/80, and their properties all satisfied the specified value. The mix design followed the standard Marshall method. Finally, 4.5% was decided as the optimal asphalt content (OAC), where the properties of AC-13 sufficiently satisfied the HMA design specification.

The wheel tracking tests were conducted at three temperatures, of 20, 40, and 60°C, three load levels of 0.44, 0.66, and 1.24kN, and two kinds of slab thickness of 40 and 60mm, namely, eighteen different conditions. The tire-specimen contact pressure for the three different load levels were, respectively, 0.56, 0.72, and 1.10MPa, which were calculated by dividing the loads by the corresponding load area measured.

The same asphalt and aggregate materials were used to prepare the specimens for the SUPT test and resilient modulus test. The number of fabricated specimens for the wheel tracking test, SUPT test and resilient modulus test was three, four and five, respectively, and the average of parallel test results was adopted for each test. Prior to testing, all the specimens in the three tests were held in an environmental chamber for at least five hours to reach temperature thermal equilibrium. The wheel tracking test results are shown in Fig. 6. At higher temperature of 40 and 60°C, all specimens exhibit remarkable deformation while little deformation is found at 20°C. Just as stated in the previous section, pronounced differences of deformation evolution are also observed for different asphalt mixtures or under different load levels. The results of shear strength and resilient modulus in MPa are presented in Table 2. The shear

**Table 2.** Modulus and Shear Strength for Evaluated Asphalt Mixtures.

Mix type	AC-13	Type A	Type B	Type C	Type D
Resilient modulus (MPa)	1787	1842	1633	1600	1912
Shear strength (MPa)	1.063	1.152	0.984	0.861	1.463

stress (MPa) in the specimens of wheel tracking test determined by FEM are illustrated in Table 3.

#### **Determination of Prediction Model by Optimization Analysis**

An optimization process was implemented to determine the coefficients of the rutting prediction model, by comparing the measured from wheel tracking test and the predicted calculated by rutting prediction model at the same input position and then finding the minimum error possible between predicted and observed responses for each data point. The error was calculated as the difference between the predicted and observed values as shown in Eq. (8):

$$\varepsilon_i = predicted_i - measured_i \tag{8}$$

There were two considerations during the optimization process: the sum of the squared error should be minimized and the sum of errors should equal to zero as shown in Fig. 7. To this end, Evolver (Genetic, Algorithm), a non-Linear optimization tool working in Excel was used. In this case, each data point corresponded to a rutting depth, a temperature, a stress as well as a strength. Inputting all data into evolver, the final model is determined as Eq. (9). This model is highly significant evidenced by higher value of determined coefficient up to 0.918.

$$RD = \sum_{i=1}^{n} 10^{-5.542} \cdot T_i^{2.524} \cdot \left\{ \frac{0.58}{V} \cdot N_V \right\}^{0.752 \left( \frac{\overline{\tau_i}}{|\tau|_i} \right)^{0.468}}$$
(9)

## Validation of Prediction Model Using Additional Asphalt Mixtures

Further laboratory wheel tracking tests were carried out to demonstrate the Eq. (9) through the participation of additional four asphalt mixtures, represented by the symbols, Mix Types A, B, C and D. The same asphalt with AC-13 was used for Mix Types A, B and C and the aggregates were replaced by limestone. Mix Type D, a kind of stone mastic asphalt (SMA) mixture, was prepared using modified asphalt as asphalt binder, fibers of 0.4% as a stabilizer and basalt as aggregate. All the above-mentioned materials, including

**Table 3.** Shear Stress in the Wheel Tracking Slab (MPa).

Slab	Sub-layer	Tire-specimen contact pressure					
thickness	Sub-layer	0.56 MPa	IPa         0.72 MPa           44         0.2475           54         0.2264           83         0.1626           82         0.1335           93         0.2395           02         0.2184           99         0.1498           35         0.1114           23         0.0948           63         0.2348           74         0.2140           60         0.1438           73         0.1019           22         0.0795	1.10 MPa			
	0~1 cm	0.2044	0.2475	0.3558			
4cm	$1\sim2$ cm	0.1554	0.2264	0.3821			
4011	$2\sim3$ cm	0.1083	0.1626	0.2890			
	$3\sim4$ cm	0.0882	0.72 MPa         1.10 MI           0.2475         0.355           0.2264         0.382           0.1626         0.289           0.1335         0.241           0.2395         0.341           0.2184         0.367           0.1498         0.266           0.1114         0.201           0.0948         0.172           0.2348         0.332           0.2140         0.359           0.1438         0.255           0.1019         0.184           0.0795         0.145	0.2411			
	$0\sim1$ cm	0.1993	0.2395	0.3414			
	$1\sim2$ cm	0.1502	0.2184	0.3676			
5cm	$2\sim3$ cm	0.0999	0.1498	0.2662			
	$3\sim4$ cm	0.0735	0.1114	0.2017			
	$4\sim5$ cm	0.0623	0.0948	0.1729			
	$0\sim1$ cm	0.1963	0.2348	0.3327			
	$1\sim2$ cm	0.1474	0.2140	0.3597			
6cm	$2\sim3$ cm	0.0960	0.1438	0.2552			
ociii	$3\sim4$ cm	0.0673	0.1019	0.1845			
	$4\sim5$ cm	0.0522	0.0795	0.1453			
	5∼6 cm	0.0457	0.0698	0.1281			

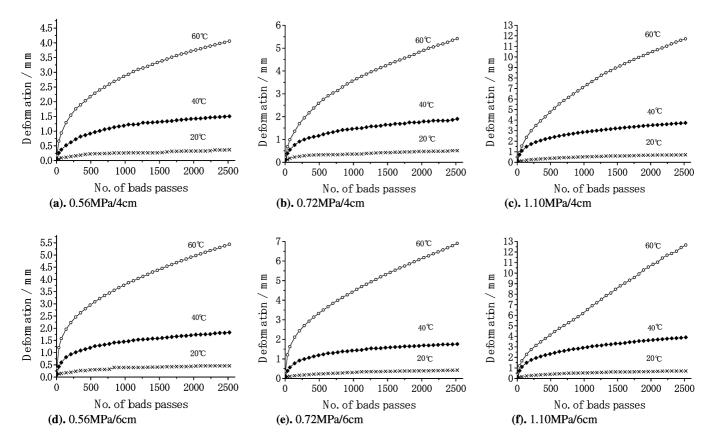


Fig. 6. Results of Wheel Tracking Tests under Different Temperatures and Pressures.

asphalt and aggregate, met the required values. The OAC for the three mixtures was 4.2, 4.4, and 4.0%, respectively, decided by the Marshall mix design method. Mix Type D has a higher OAC content of 6.2%. The volumetric properties of all four mixtures at OAC also satisfied the requirement. The specimens for each mixture were prepared to the thickness of 50mm and tested at 40 and 60°C, respectively. Mix Type A was subjected to testing at varying pressures of 0.56, 0.72, and 1.10MPa, and Mix Types B, C, and D were only examined at a constant pressure of 0.72MPa.

The shear strength and resilient modulus of Mix Types A, B, C, and D, and shear stresses in the wheel tracking slab are presented in Table 2 and 3, respectively. The comparisons between the measured from wheel tracking test and the predicted calculated from Eq. (9) for Mix Types A, B, C, and D are shown in Fig. 8 and Fig. 9.

For Mix A, the predicted gives a comparable value to the measured when changing the temperature and contact pressure, except for the case of 1.10MPa and 60°C, at which the measured is significantly higher than the predicted. This is because some of the large aggregates have been compacted to fracture leading to greater deformation. For Mix Types B, C, and D, though there exist some differences between the measured and the predicted, the average agreement over time seems acceptable, which indicates that the model is suitable for different asphalt mixtures or different pressures within 2520 load passes.

In summary, Eq. (9) can provide a satisfactory result to predict deformation for different asphalt mixtures under varying conditions in the laboratory test.

## **Calibration of Rutting Prediction Model**

Although Eq. (9) can closely estimate the rutting in the wheel tracking test, the ultimate objective is to apply the predictive model to the "real roads". But the gap existing between the laboratory and the field prevents the extensive utilization of this model. Some calibrations are indispensable to shift the model from the laboratory to the pavement.

In this study, a full-scale cyclic pavement test (FSCDT), which can provide confirmative evidence for laboratory tests, was used to calibrate the laboratory model. The pavement structure is shown in Table 4. The test conditions were described as below: temperature of pavement surface, 55°C; axle load, 27.5kN; tire pressure, 0.70MPa; loading speed, 40km/h; length of road, 33m.

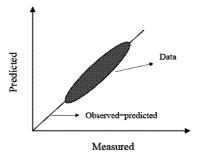


Fig. 7. Optimization Target for Calibration.

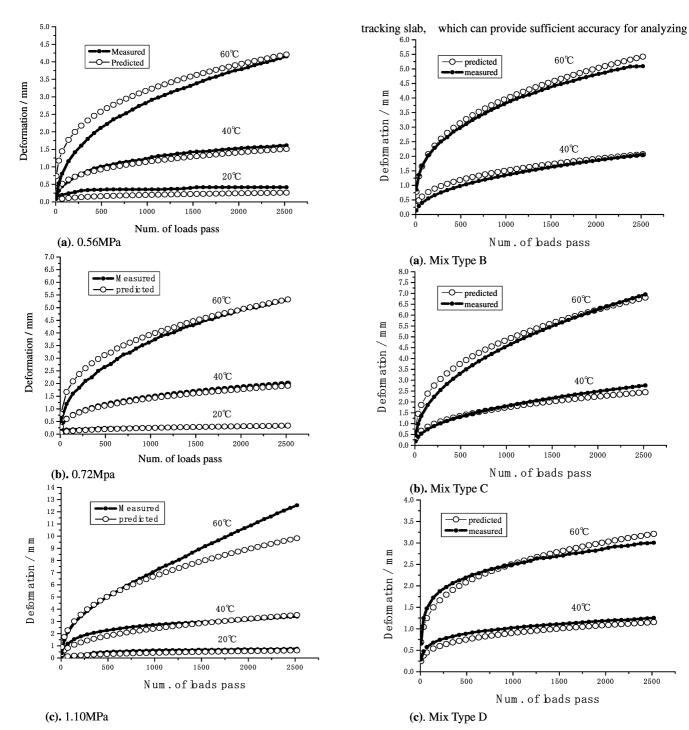


Fig. 8. Comparison between Measured and Predicted Rut Depths of Mix type A.

Although there was a minor difference between the accelerated pavement test and pavement in situ, the mechanisms of rutting in full-scale cyclic pavement were almost identical to those in situ (Fig. 10). In this test, more than 98% of the total deformation was within the asphalt layer. The resilient modulus, shear strength of all materials and shear stress were listed in Table 5 and 6, respectively. The FEM model for FSCDT was 5m long, 5m wide, and 8m deep in foundation. Boundary conditions were the same as that of the wheel

Fig. 9. Comparison between Measured and Predicted Rut Depths of Mix type B, C, and D.

the shear stress in pavement. The temperature in FSCDT pavement followed the same pattern with that in place, which was measured and listed in Table 7. It is worth noting that horizontal force as a consequence of acceleration or deceleration. Evolver was employed to implement the optimization process. After finishing this calibration step, Eq. (9) becomes:

$$RD = \sum_{i=1}^{n} 10^{-5.881} \cdot T_i^{2.512} \cdot \left\{ \frac{0.58}{V} \cdot N_V \right\}^{0.743 \cdot \left(\frac{\tau_i}{\tau_{0i}}\right)^{0.472}}$$
(10)

2500

2500

Table 4. Pavement Structure in Full Scale Cyclic Pavement Test.

Layer		Materials type	•
thickness (mm)	Mixture		Mixture
40	HMA wearing course	40	HMA wearing course
80	HMA binder course	80	HMA binder course
150	HMA base course	150	HMA base course
360	cement stabilized gravel	360	cement stabilized gravel
	foundation		foundation

**Table 5.** Material Properties in Full Scale Cyclic Pavement.

	Titatellal I I	operates in	I all bear	e ejemera	· CIIICIIC.
Materials	Wearing course	Binder course	Base course	Cement stabilized] gravel	Foundation
Resilient modulus (MPa)	2000	1900	2223	15000	45
Poisson ratio	0.35	0.35	0.35	0.20	0.40
Shear strength (MPa)	1.261	0.943	0.797		

**Table 6.** Shear Stress in Full Scale Cyclic Pavement (MPa).

Sub-layer (cm)	Shear stress	Sub-layer (cm)	Shear stress	Sub-layer (cm)	Shear stress
0~1	0.1102	9~10	0.2033	18~19	0.1158
1~2	0.2110	10~11	0.1908	$19 \sim 20$	0.1093
2~3	0.2538	11~12	0.1790	20~21	0.1026
3~4	0.2633	12~13	0.1685	$21 \sim 22$	0.0971
4~5	0.2611	13~14	0.1593	$22 \sim 23$	0.0916
5~6	0.2527	$14 \sim 15$	0.1501	$23 \sim 24$	0.0870
6~7	0.2422	15~16	0.1406	$24 \sim 25$	0.0827
<b>7∼</b> 8	0.2295	16~17	0.1316	$25 \sim 26$	0.0792
8~9	0.2165	17~18	0.1237	26~27	0.0763

Fig. 11 shows the plot of the predicted rutting depth and the measured rutting depth, and the higher determined coefficient of 0.94, indicating that Eq. (10) is reliable. But in essence, Eq. (10) should be called a deformation prediction model because it is decided by the compressive deformation. In other words, rutting not only includes compressive deformation but also neighboring upheave at both sides (Fig. 12). Therefore, by comparing the compressive deformation and rutting measured in the FSCDT test, an upheave coefficient of 0.45 calculated by dividing the difference between rutting and deformation by deformation is put forward. After introducing the upheave coefficient, the final expression of the rutting model can be described as Eq. (11).

$$RD = 1.45 \cdot \sum_{i=1}^{n} 10^{-5.881} \cdot T_i^{2.512} \cdot \left\{ \frac{0.58}{V} \cdot N_V \right\}^{0.743 \cdot \left(\frac{\tau_i}{\tau_{0i}}\right)^{0.472}}$$
(11)

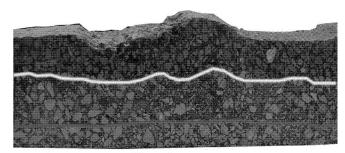


Fig. 10. Trench in Full Scale Cyclic Pavement Test.

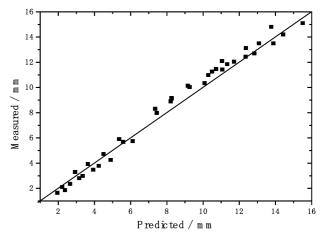


Fig. 11. Measured Deformation versus Predicted Deformation.

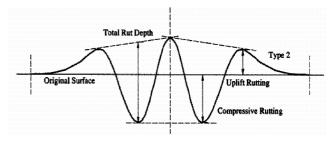


Fig. 12. Comparison between Rutting and Deformation.

## **Conclusions**

This study presented a developed method for predicting rutting in asphalt pavements, based on the most widely used empirical model. Its most significant enhancement was the introduction of the shear concept realized by the Static Uniaxial Penetration Test and FEM analysis, which provided a stronger foundation for integrating pavement structure and materials design into an integral mechanistic-empirical framework. This new approach considered traffic and environmental characteristics as well as pavement structure and materials properties, and the predicted from this model can match the measured well through the rutting history for different asphalt mixtures when subjecting to various test conditions. Furthermore, the suitability of this rutting prediction model, by taking into account the upheave coefficient and temperature gradient, was improved after calibration using the results obtained from full scale cyclic pavement tests.

Depth(cm)	0.5	1.5	2.5	3.5	4.5	5.5	6.5	7.5	8.5	9.5
Temperature(°C)	59.4	59.1	58.9	58.5	58.2	57.8	57.4	57.0	56.6	56.1
Depth(cm)	10.5	11.5	12.5	13.5	14.5	15.5	16.5	17.5	18.5	19.5
Temperature(°C)	59.4	59.1	58.9	58.5	58.2	57.8	57.4	57.0	56.6	56.1
Depth(cm)	20.5	21.5	22.5	23.5	24.5	25.5	26.5	27.5	28.5	29.5
Temperature(°C)	50.5	49.9	49.4	48.9	48.4	47.9	47.4	46.9	46.4	46.0
Depth(cm)	30.5	31.5	32.5	33.5	34.5	35.5	36.5	37.5	38.5	39.5
Temperature(°C)	45.6	45.2	44.8	44.4	44.1	43.8	43.5	43.3	43.1	42.9

Without question, considerable efforts are needed to assess this new rutting model before it is applied to the "real road" and included in the pavement design guide, although this method looks very promising. A filed demonstration, the essential but complicated step, is currently being undertaken to shift the model from the laboratory to the real road in Tongji University. In addition, a related design index to control rutting, referred to  $\tau$  /  $\tau$  0, is hoped to be proposed from this rutting prediction model in the future.

## Acknowledgements

The authors would like to express their sincere thanks to the National Science Foundation for Distinguished Young Scholars of China for funding this research project (Grant No. 50325825). Special thanks are also extended to Dr. Zhou Gang, who provided the data measured in accelerated pavement test.

## Disclaimer

The information presented in this paper only reflects the views of the authors. No official endorsement should be associated with the information provided.

## References

- 1. Archilla, A.R. and Madanat, S. (2000). Development of Asphalt Pavement Rutting Model from Experimental Data, *Journal of Transportation Engineering (ASCE)*, 126(4), pp. 291-299.
- National Cooperative Highway Research Program (NCHRP). (2004). Guide for Mechanistic-Empirical Design of New and Rehabilitated Pavement Structures, NCHRP 1-37A Report, Chapter 3: Design new and reconstructed flexible pavement, pp. 46-56, ERES division of ARA Inc., Champaign, Illinois, USA.
- 3. Hofstra, A. and Klompa, J. (1972). Permanent Deformation of Flexible Pavements under Simulated Road Traffic Conditions, *Proceedings of the Third International Conference on the Structural Design of Asphalt Pavements*, London, United Kingdom, pp. 613-621.
- Eisenmann, J. and Hilmer, A. (1987). Influence of Wheel Load and Inflation Pressure on the Rutting Effect at Asphalt Pavement Experiments and Theoretical Investigations, Proceedings of the Sixth International Conference on the Structural Design of Asphalt Pavements, Ann Arbor, USA, 1, pp. 392-403.
- Sousa, J.B., Craus, J., and Monimith, C.L. (1994). Summary Report on Permanent Deformation on Asphalt Concrete,

- Report SHRP-A-318, Strategic Highway Research Program, National Research Council, Washington D.C., USA, pp.40-60.
- Myers, L.A., Drakos, C., and Roque, R. (2002). The Combined Effects of Tire Contact Stresses and Environment on Surface Rutting and Cracking Performance, *Proceedings of the Ninth International Conference on Asphalt Pavements*, Washington. D.C., USA, 3, pp. 31-40.
- 7. Mohamed, M.E., Witczakm, M.W., and Sherif, E. (2005). Verification for the Calibrated Permanent Deformation Models for the 2002 Design Guide, *Journal of the Association of Asphalt Paving Technologists*, 74, pp. 521-571.
- 8. McLeod, N. W. (1950). A Rational Approach to the Design of Bituminous Paving Mixtures, *Journal of the Association of Asphalt Paving Technologists*, 19, pp. 82–87.
- Fwa, T. F., Tan, S. A., and Zhu, L. Y. (2004). Rutting Prediction of Asphalt Pavement Layer Using C-φ Model, *Journal of Transportation Engineering (ASCE)*, 130 (5), pp.676-683.
- 10. Monismith, C. L., Popescu, L., and Harvey, J. T. (2006). Use of Shear Test Data for Mix Design, Performance Analysis and Rut Depth Prediction, *Proceedings of the Tenth International Conference on the Structural Design of Asphalt Pavements*, Ouebec, Canada, CD-ROM.
- 11. Sun, L.J., Hu, X.D., Bi, Y.F., Hu, X., and Li, F. (2006). Top-down Cracking Analysis and Control for Asphalt Pavements, *Proceedings of the Tenth International Conference on the Structural Design of Asphalt Pavements*, Quebec, Canada, CD-ROM.
- Sousa, J.B., Leahy, R.B., Harvey, J., and Monismith, C.L. (1994). Permanent Deformation Response of Asphalt Aggregate Mixes, SHRP-A-415, Strategic Highway Research Program, Transportation Research Board, National Research Council, Washington D.C., USA, pp. 17-22.
- Harold, L. and Von, Q. (1994). Performance Prediction Models in the Superpave Mix Design System. SHRP-A-699, Strategic Highway Research Program, Transportation Research Board, National Research Council, Washington D.C., USA, pp.53-57.
- Hao, P. and Hachiya, Y. (2004). Study on Performance and Test Methods of Asphalt Mixtures for Airport Pavements, *Technical Note, No. 177*, National Institute for Land and Infrastructure Management, Yokosuka, Japan, pp. 15-23.
- 15. Su, K. (2006). Mechanism and Prediction of Rutting in Asphalt Pavements, *Ph.D. Dissertation, School of Transportation Engineering*, Tongji University, Shanghai, China, pp.60-80.
- Margarita, R., Mehdi, O.H., and Dumont, A.G. (2006). New Predictive Method for Evaluation of Pavement Rutting, Proceeding of the Tenth International Conference on the Structural Design of Asphalt Pavements, Quebec, Canada, CD-ROM.
- 17. Guo, D.Z. and Ren, R.B. (2001). Visco-Elastic Mechanics in Multi-Layered Pavements, *Ha'er Bin Technology*

- University Press, Ha'er Bin, China. pp. 133-135.
- 18. Pell, P. S. and Taylor, I. F. (1968). Asphaltic Road Materials in Fatigue. Journal of the Association of Asphalt Paving Technologists, 38, pp. 371-423.
- 19. Carpenter, S.H. (1993). Permanent Deformation: Field Evaluation, Transportation Research Record, No.1417, pp. 135-143.
- 20. The test specifications for asphalt and asphalt mixtures (JTJ052). (2000). People communication press. (in Chinese)
- 21. Hao, P. and Hachiya, Y. (2004). Evaluation Indicator of Asphalt Mixture Rutting Susceptibility, Journal of testing and

- evaluation, 32(3), pp. 194-201.
- 22. Sun, L.J. (2004). Asphalt Pavement Structure Behavior Theory, People communication press., Beijing, China, pp. 101-130.
- 23. Bi, Y. (2004). Research on Shear Test Method of Asphalt Mixture, Ph.D. Dissertation, School of Transportation Engineering, Tongji University, Shanghai, China. pp. 53-64.
- 24. Chen, X.W., Huang, B.S., and Xu, Z.H. (2006). Uniaxial Penetration Testing for Shear Resistance of Hot Mix Asphalt Mixtures, TRB annual meeting, Washington. D.C., USA, CD-ROM.